

Spin current and shot noise from a quantum dot coupled to a quantized cavity field

Ivana Djuric and Chris P. Search

*Department of Physics and Engineering Physics,
Stevens Institute of Technology, Hoboken, NJ 07030*

(Dated: July 4, 2018)

We examine the spin current and the associated shot noise generated in a quantum dot connected to normal leads with zero bias voltage across the dot. The spin current is generated by spin flip transitions induced by a quantized electromagnetic field inside a cavity with one of the Zeeman states lying below the Fermi level of the leads and the other above. In the limit of strong Coulomb blockade, this model is analogous to the Jaynes-Cummings model in quantum optics. We also calculate the photon current and photon current shot noise resulting from photons leaking out of the cavity. We show that the photon current is equal to the spin current and that the spin current can be significantly larger than for the case of a classical driving field as a result of cavity losses. In addition to this, the frequency dependent spin (photon) current shot noise show dips (peaks) that are a result of the discrete nature of photons.

PACS numbers: 42.50.Pq,73.63.Kv,78.67.Hc

I. INTRODUCTION

The field of spintronics has emerged as a new field in which the spin degrees of freedom of charge carriers in solid state devices are exploited for the purpose of information processing. Manipulation of the spin degrees of freedom rather than the charge has the advantage of longer coherence and relaxation times¹. In contrast to spin-polarized charge currents², pure spin currents, $I_s = s(I_\uparrow - I_\downarrow)$, are the result of an equal number of spin up (\uparrow) and spin down (\downarrow) charge carriers moving in the opposite direction so that the charge current, $I_c = q(I_\uparrow + I_\downarrow)$, is zero. Here, I_σ are the particle currents for each spin projection, $s = \hbar/2$ the spin of the particles, and q the charge of the carriers.

There have been a number of proposals for generating spin currents in semiconductor nanostructures, which include spin-orbit (SO) dependent scattering off impurities (the extrinsic Spin-Hall effect)³, and the intrinsic spin hall effect in doped semiconductors⁴ where the energy bands are split due to spin orbit coupling⁵. Interference between one and two photon optical absorption in a semiconductor can also be used to excite a pure spin current⁶. A quantum spin pump created by periodic shape deformations of an open quantum dot⁷ has been proposed theoretically and also demonstrated experimentally⁸. Quantum spin pumps based on periodic variations of external potentials applied to a quantum wire have also been proposed⁹. Additional proposals include quantum pumps that use independent variations of localized magnetic fields in a two-dimensional electron gas¹⁰, a quantum dot spin turnstile¹¹, classical incoherent spin pumping¹², and the use of superconducting leads¹³.

Electron spin resonance (ESR) in a quantum dot connected to leads has been proposed as a way to generate a pure spin current when there is a large Zeeman splitting^{14,15}. The spin current and spin shot noise generated by such a quantum dot spin battery has been analyzed by several groups^{15,16,17}. In previous work on this

spin battery, a classical electromagnetic (e.m.) field was used to induce the spin flips. However, from quantum optics we know that the Jaynes-Cummings model, which describes the interaction of a two-level atom with a single mode of the quantized e.m. field exhibits behavior not present when using a classical field¹⁹. This includes collapse and revivals in the amplitude of Rabi oscillations caused by the discrete nature of the photon number and the ability to create non-classical states of the e.m. field as is done with the micromaser¹⁹.

The intensity correlations of the e.m. field have been of central importance in quantum optics for decades because they reveal important information about the quantum state of the field that is not present in the average intensity such as anti-bunching, a purely non-classical effect, first observed in resonance fluorescence²⁰. More recently, the study of the current shot noise, which is given by the current-current correlator, has become the subject of intense theoretical study in mesoscopic physics. This is because the shot noise contains information about the quantum statistics of the charge carriers, the interactions between particles, and the device structure that is not present in measurements of the conductance¹⁸. For example, the Pauli effect reduces the zero frequency charge current noise below the Schottky value, $2e\langle I_c \rangle$, corresponding to anti-bunching. However, it is difficult to discriminate the effect of the Pauli principle and interparticle interactions in the charge noise. Since the Pauli exclusion principle does not effect fermions of opposite spin, the shot noise in the spin current is a much more sensitive probe of the interactions between particles¹⁶. In many respects, the current shot noise is the direct analogue of the second order intensity correlations of the e.m. field.

Here we extend the model of the quantum dot spin battery^{14,15} by studying for the first time the use of a quantized cavity field to induce spin flips between Zeeman states. We analyze the spin current and spin current shot noise and find that the current produced by

the quantum field can be larger than that produced by a classical field. Moreover, the frequency dependent spin shot noise shows unambiguous signatures of the discrete nature of the photon states of the cavity.

In the section II, we develop our theoretical model in detail. Section III discusses our numerical and analytic results for spin current and shot noise. Finally, in section IV, we conclude with a few comments on the experimental prospects for our work.

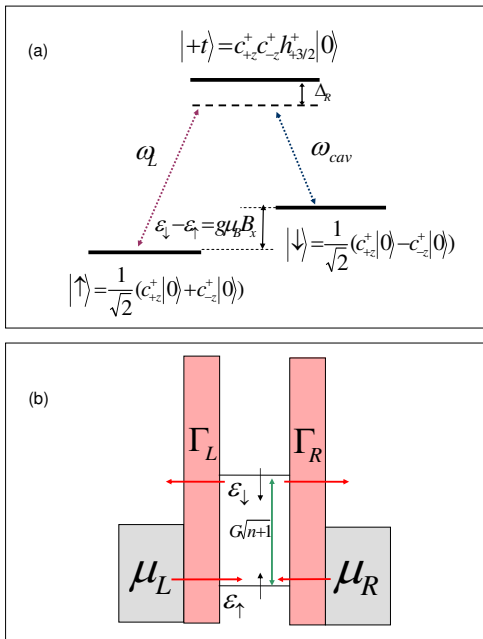


FIG. 1: (a) Raman transition between the electronic Zeeman states, $|\uparrow, \downarrow\rangle$, via an intermediate trion state, $|+t\rangle$, induced by a laser with frequency ω_L and a cavity mode with frequency ω_{cav} . The spin eigenstates along the direction of the magnetic field are superpositions of spin eigenstates in the growth direction, $\hat{c}_{\pm z}^\dagger|0\rangle$. (b) Diagram of quantum dot indicating Zeeman energy levels in the dot and allowed tunnelling between leads and dot.

II. MODEL

For our quantum field spin battery, the quantum dot is embedded in a high-Q microcavity. Strong coupling between an individual quantum dot and a single mode of an optical microcavity has recently been achieved^{21,22}. Although electron transport through quantum dots is most commonly studied using electrically defined quantum dots in two dimensional electron gases²³, these dots are not well suited for optical experiments because of the strong optical absorption of the metal electrodes used to define the dots²⁴. Self-assembled quantum dots, as used in Ref. 21, are readily studied using optical techniques and in addition there have been several experimental studies of electron transport including shot noise

through individual and coupled pairs of self-assembled InAs quantum dots^{25,26,27}. Along a similar line, the ability to control the tunnelling of electrons or holes between self-assembled dots and a doped GaAs reservoir by a gate voltage combined with simultaneous spectroscopic studies of these charged quantum dots has been demonstrated^{28,29}. For the sake definiteness, we therefore assume that the quantum dot under consideration is a self-assembled dot such as an InAs dot embedded in GaAs.

There are two electron reservoirs at chemical potential, μ , that are coupled to the dot via tunnelling. (None of the results presented here require two leads coupled to the dot. The only difference between the two lead and one lead case being the total rate at which electrons tunnel into or out of the dot since it is the sum of the tunnelling rates from each lead.) Only a single empty orbital energy level, ϵ_D , of the dot lies close to μ . The Zeeman splitting between the two electron spin states is $\Delta = \epsilon_\downarrow - \epsilon_\uparrow = g_x \mu_B B$ where B is a static magnetic field along the x-axis that is perpendicular to the growth direction (z). μ_B is the Bohr magneton and g_x is the electronic g-factor along the direction of the magnetic field. The energy levels satisfy $\epsilon_\uparrow = \epsilon_D - \Delta/2 < \mu < \epsilon_\downarrow = \epsilon_D + \Delta/2$ so that only spin up electrons can tunnel into the dot and only spin down electrons can tunnel out³⁰. In the limit of infinite Coulomb Blockade that we consider, only a single electron can occupy the dot resulting in the bare Hamiltonian for the dot, $H_D = \epsilon_\uparrow \hat{c}_\uparrow^\dagger \hat{c}_\uparrow + \epsilon_\downarrow \hat{c}_\downarrow^\dagger \hat{c}_\downarrow$ where \hat{c}_σ (\hat{c}_σ^\dagger) are annihilation (creation) operators for electrons in the dot with spin σ in the x-direction of the magnetic field.

Transitions between different spin states of the conduction band electron in the dot are induced via a two-photon Raman transition involving a strong laser field that may be treated classically and a quantized mode of the microcavity similar to Ref. 31. The two optical fields couple the electron spin states to a higher energy charged exciton state (known as a trion) by creating an additional electron-hole pair in the dot³². Recent experiments have shown how Raman scattering via intermediate trion states can be used to generate electron spin coherence^{33,34} and to pump the electron spin into a specific spin state²⁹.

The lowest energy trion states excited by σ^+ and σ^- polarized light consist of an electron singlet with a heavy hole, $|+t\rangle = \hat{c}_\uparrow^\dagger \hat{c}_\downarrow^\dagger \hat{h}_{+3/2}^\dagger |0\rangle$ and $|-t\rangle = \hat{c}_\uparrow^\dagger \hat{c}_\downarrow^\dagger \hat{h}_{-3/2}^\dagger |0\rangle$ where $\hat{h}_{\pm 3/2}^\dagger$ are heavy hole creation operators with spin projections $\pm \hbar 3/2$ along the z-axis and $|0\rangle$ is the empty dot state. The σ^+ polarized laser with frequency ω_l and Rabi frequency Ω_l couples each of the electron spin states to the $|+t\rangle$ trion state. On the other hand, the x-polarized cavity field with vacuum Rabi frequency g_{cav} and frequency ω_c couples the spin states to both the $|+t\rangle$ and $|-t\rangle$ states. When the two fields are far detuned from the creation energy for the trions, the intermediate trion states can be adiabatically eliminated to give the Hamil-

tonian,

$$H_{cav} = \hbar\omega_c \hat{a}^\dagger \hat{a} + G(\hat{a}^\dagger \hat{c}_\uparrow^\dagger \hat{c}_\uparrow e^{-i\omega_l t} + h.c.). \quad (1)$$

where \hat{a} is a bosonic annihilation operator for the cavity field. Here $G = g_{cav}\Omega_l/4\Delta_R$ and Δ_R is the detuning of the laser and cavity mode from the $|+t\rangle$ creation energy. AC stark shifts of the electron energy levels due to the optical fields have been absorbed into a redefinition of ϵ_σ .

By transforming to a rotating frame for the electron operators, $\hat{c}_\uparrow = \hat{C}_\uparrow \exp(i\omega_l t/2)$ and $\hat{c}_\downarrow = \hat{C}_\downarrow \exp(-i\omega_l t/2)$ the explicit time dependence is removed from H_{cav} and H_D becomes,

$$H'_D = \epsilon_D(\hat{C}_\uparrow^\dagger \hat{C}_\uparrow + \hat{C}_\downarrow^\dagger \hat{C}_\downarrow) + (\Delta - \omega_l)(\hat{C}_\downarrow^\dagger \hat{C}_\downarrow - \hat{C}_\uparrow^\dagger \hat{C}_\uparrow)/2. \quad (2)$$

Since $\Delta < \omega_l$ for optical frequencies and typical Zeeman splittings, the energies of the spin states are inverted in the rotating frame. The two-photon resonance can then be seen to be $\omega_{cav} = \omega_l - \Delta$. This level inversion coincides with H_{cav} where one sees that the $|\uparrow\rangle \rightarrow |\downarrow\rangle$ transition creates photons. Energy is in fact conserved in this process because the energy for the spin flip and the cavity photon comes from the laser field, which is treated in the undepleted pump approximation. $H_{cav} + H'_D$ is the Jaynes-Cummings Hamiltonian, which results in independent time evolution for each of the two-state manifolds $\{|\uparrow, n\rangle, |\downarrow, n+1\rangle\}$ characterized by the photon number n . Coupling between these manifolds is a result of the dot-lead coupling and the cavity damping.

The coupling between the lead and the dot can be treated using a master equation similar to the one developed in Ref. 35. We define the matrix elements of the dot-cavity density operator to be $\rho_{\sigma,\sigma'}^{(n,m)} = \langle n, \sigma | \hat{\rho} | \sigma', m \rangle$ where $|\sigma, n\rangle$ represents a state with n photons in the cavity and $\sigma = 0, \uparrow, \downarrow$ corresponding to no electrons, one spin up, or one spin down electron, respectively. The specific form of the master equations for the lead coupling are

$$\dot{\rho}_{0,0}^{(n,m)}|_{lead} = \Gamma_\downarrow^{(-)} \rho_{\downarrow,\downarrow}^{(n,m)} - \Gamma_\uparrow^{(+)} \rho_{0,0}^{(n,m)} \quad (3)$$

$$\dot{\rho}_{\uparrow,\uparrow}^{(n,m)}|_{lead} = \Gamma_\uparrow^{(+)} \rho_{0,0}^{(n,m)} \quad (4)$$

$$\dot{\rho}_{\downarrow,\downarrow}^{(n,m)}|_{lead} = -\Gamma_\downarrow^{(-)} \rho_{\downarrow,\downarrow}^{(n,m)} \quad (5)$$

$$\dot{\rho}_{\uparrow,\downarrow}^{(n,m)}|_{lead} = -\Gamma_\downarrow^{(-)} \rho_{\uparrow,\downarrow}^{(n,m)}/2. \quad (6)$$

The rate at which spin up electrons tunnel into the dot is given by $\Gamma_\uparrow^{(+)} = \sum_\eta \Gamma_{\uparrow,\eta}^{(+)} = 2\pi \sum_\eta \sum_k |t_{\eta,k,\uparrow}|^2 \delta(\omega - \epsilon_{\eta,k,\uparrow}) f_\eta(\epsilon_\uparrow)$ where $f_\eta(\omega)$ is the Fermi distribution for the leads and $t_{\eta,k,\sigma}$ is the tunnelling amplitude for an electron from lead η with momentum $\hbar k$, spin σ , and energy $\epsilon_{\eta,k,\sigma}$. $\Gamma_\downarrow^{(-)} = \sum_\eta \Gamma_{\downarrow,\eta}^{(-)} = 2\pi \sum_\eta \sum_k |t_{\eta,k,\downarrow}|^2 \delta(\omega - \epsilon_{\eta,k,\downarrow})(1 - f_\eta(\epsilon_\downarrow))$ is the rate at which spin down electrons tunnel out of the dot.

Since the pump laser interacting with the quantum dot is a source of energy for the cavity field, the photons in the cavity field would increase without bound and not reach a steady state in the absence of cavity damping.

In order to describe the damping of the cavity we use a zero temperature ($k_B T \ll \hbar\omega_{cav}$) Born-Markov master equation with the matrix elements¹⁹,

$$\begin{aligned} \dot{\rho}_{\sigma,\sigma'}^{(n,m)}|_{cavity} &= -\Gamma_{cav}(n+m)\rho_{\sigma,\sigma'}^{(n,m)}/2 \\ &+ \Gamma_{cav}\sqrt{(n+1)(m+1)}\rho_{\sigma,\sigma'}^{(n+1,m+1)}. \end{aligned} \quad (7)$$

Lastly, the unitary time evolution between the dot and the cavity field is given by $\dot{\rho}_{\sigma,\sigma'}^{(n,m)}|_{d-c} = (i\hbar)^{-1} \langle n, \sigma | [H'_D + H_{cav}, \hat{\rho}] | m, \sigma' \rangle$. The complete master equation for the dot-cavity system is then given by

$$\dot{\rho}_{\sigma,\sigma'}^{(n,m)} = \dot{\rho}_{\sigma,\sigma'}^{(n,m)}|_{lead} + \dot{\rho}_{\sigma,\sigma'}^{(n,m)}|_{cavity} + \dot{\rho}_{\sigma,\sigma'}^{(n,m)}|_{d-c}. \quad (8)$$

For simplicity, we consider only two photon resonance, $\omega_{cav} = \omega_l - \Delta$, which is easily achieved by properly tuning the laser frequency.

We also assume that the couple between the left and right leads and the dot are the same and that the tunnelling between the leads and the dot is spin independent, $\Gamma_{\uparrow L}^{(+)} = \Gamma_{\downarrow L}^{(-)} = \Gamma_{\uparrow R}^{(+)} = \Gamma_{\downarrow R}^{(-)} = \Gamma$, where we will use Γ as our unit of energy from here on. Although there have been no measurements of the spin dependence of tunnelling in self assembled dots, the tunnelling rates in electrically defined quantum dots can be spin dependent^{36,37}. However, our numerical results indicate that as long as $\Gamma_{\uparrow L}^{(+)} + \Gamma_{\uparrow R}^{(+)}$ is similar in size to $\Gamma_{\downarrow L}^{(-)} + \Gamma_{\downarrow R}^{(-)}$, the results presented here for equal spin tunnelling rates will show no significant difference from case of unequal tunnelling rates.

III. RESULTS

Due to the identical coupling to both leads, the currents will be the same in both leads, $I_{L,\sigma} = I_{R,\sigma} = I_\sigma$ where $I_{\eta,\uparrow(\downarrow)}$ is the spin-up(down) electron particle current in the lead $\eta = L, R$. The average spin current, $I_s = s(I_{\eta,\uparrow} - I_{\eta,\downarrow})$, is then independent of the lead with the stationary currents given by $I_\uparrow = \Gamma\bar{\rho}_{0,0}$ and $I_\downarrow = -\Gamma\bar{\rho}_{\downarrow,\downarrow}$ ³⁸. Here, the over bar denotes the steady state solution and in particular $\bar{\rho}_{i,i} = \sum_n \rho_{i,i}^{(n,n)}$ is the steady state solution of Eq. 8 traced over the state of the cavity. It is easy to show that $\bar{\rho}_{\downarrow,\downarrow} = \bar{\rho}_{0,0}$. It then follows from Eq. (8) that the spin current can be expressed as

$$I_s = 2s\Gamma\bar{\rho}_{\downarrow,\downarrow} = siG \sum_n \sqrt{n}(\bar{\rho}_{\downarrow,\downarrow}^{(n,n-1)} - \bar{\rho}_{\uparrow,\downarrow}^{(n-1,n)}) \quad (9)$$

The photon current leaving the cavity is given by $I_{photon} = \Gamma_{cav}\langle n_{cav} \rangle$ where $\langle n_{cav} \rangle = \sum_{\sigma,n} n \bar{\rho}_{\sigma,\sigma}^{(n,n)}$ is the average number of photons inside the cavity. In the steady state one finds using Eq. 9 that $I_{photon} = I_s/s$.

The equality of the spin and photo-current is because exactly one photon is created in the cavity for every electron that transits through the dot contributing to the net spin current. In the steady state, the rate at which

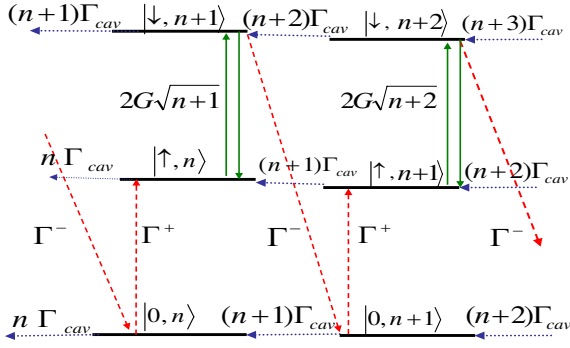


FIG. 2: Transitions between states $|\sigma, n\rangle$ with the rates for each transition. Here $\sigma = 0, \uparrow, \downarrow$ is the dot state and n the photon number in the cavity

photons are lost from the cavity must exactly balance the rate at which photons are created by electron spin flips in the dot. As a result, it would be possible to measure the spin current, which is usually a difficult task, by measuring the photo-current or, to measure the creation of one photon states inside the cavity by measuring the charge state of the dot, which can be done with an adjacent quantum point contact³⁹.

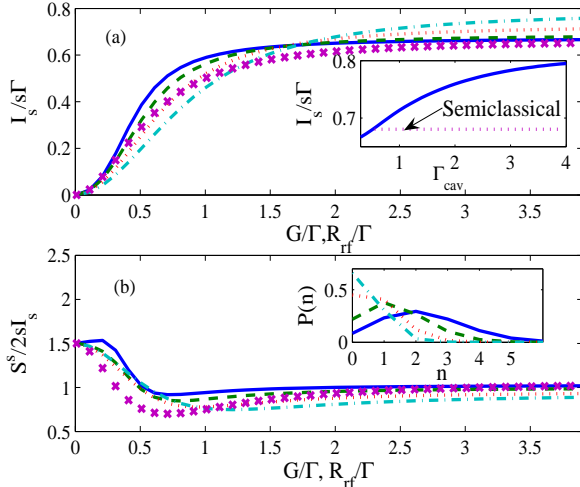


FIG. 3: (a) Spin current and (b) zero frequency shot noise vs. Rabi frequency calculated for different cavity decay rates: solid line ($\Gamma_{cav} = 0.3\Gamma$), dashed line ($\Gamma_{cav} = 0.5\Gamma$), dotted line ($\Gamma_{cav} = \Gamma$), dashed-dot line ($\Gamma_{cav} = 2\Gamma$), and 'x's' are for the classical e. m. field. Inset of fig. 2(a) is spin current vs. cavity decay rate in units of Γ and inset of fig. 2(b) is the photon probability distribution for $G = 4\Gamma$.

In Fig. 3(a) we compare the spin current in our system with the system studied in Ref. 15 where a classical e.m. field was used to drive the transition between the different spin states. This semi-classical model can be obtained from our quantum model by making the replacement $G\hat{a} \rightarrow R_{rf}$, where R_{rf} is the classical field Rabi frequency, and by eliminating all cavity degrees of

freedom from the density operator, i.e. $\rho_{\sigma, \sigma'}^{(n, m)} \rightarrow \rho_{\sigma, \sigma'}$ and $\dot{\rho}_{\sigma, \sigma'}^{(n, m)}|_{cavity} = 0$. The semiclassical stationary solution for the spin current is $I_s = 2sR_{rf}^2\Gamma/(\Gamma^2 + 3R_{rf}^2)$. For $R_{rf} > \Gamma$ the populations saturate, $\bar{\rho}_{0,0} = \bar{\rho}_{\downarrow, \downarrow} = \bar{\rho}_{\uparrow, \uparrow} = 1/3$, leading to a maximum spin current of $2s\Gamma/3$. However, this is not the case with the quantum field for $G > \Gamma$ where the stationary populations are no longer equal, $\bar{\rho}_{0,0} = \bar{\rho}_{\downarrow, \downarrow} > \bar{\rho}_{\uparrow, \uparrow}$, which leads to a current that saturates at a value *greater* than the semiclassical value of $2s\Gamma/3$ as shown in the inset of Fig. 3(a).

The population imbalance created when $G > \Gamma$, $\bar{\rho}_{\downarrow, \downarrow} - \bar{\rho}_{\uparrow, \uparrow} > 0$, is different from what one would expect from laser theory¹⁹. For $G < \Gamma$, a 'lasing' population inversion, $\bar{\rho}_{\downarrow, \downarrow} - \bar{\rho}_{\uparrow, \uparrow} < 0$, does occur. The anomalous population difference is most easily explained for $\Gamma_{cav} \gg \Gamma$ since for increasing Γ_{cav} the anomalous population imbalance increases (inset of Fig. 3(a)). In this limit only the states $|0, 0\rangle$, $|\uparrow, 0\rangle$, $|\downarrow, 1\rangle$ and $|\downarrow, 0\rangle$ have non-negligible populations. When a spin up electron enters the dot, it undergoes a spin flip creating the state $|\downarrow, 1\rangle$ in a time $G^{-1} \ll \Gamma^{-1}$, which then quickly decays to $|\downarrow, 0\rangle$ in a time $\Gamma_{cav}^{-1} \ll \Gamma^{-1}$. The spin down electron then remains in the dot for a time $\sim \Gamma^{-1}$ after the photon has left the cavity. This time is much longer than all other time scales and represents a bottleneck preventing the creation of more photons. This gives rise to the larger population in $|\downarrow, 0\rangle$ compared to $|\uparrow, 0\rangle$. This is similar to the single atom laser where the photo-current saturated as a result of the finite time it took to recycle population in the atom⁴⁰. By contrast, when $\Gamma_{cav} \gg \Gamma > G$, the time spent in the state $|\uparrow, 0\rangle$ is longer than the lifetime of $|\downarrow, 0\rangle$. In this case one has $\bar{\rho}_{\uparrow, \uparrow} > \bar{\rho}_{\downarrow, \downarrow}$.

Additional information can be obtained by examining the shot noise for the spin current and the photon current. The noise power spectrum for the current can be expressed as the Fourier transform of the current-current correlation function,

$$S_{I_{\nu, \sigma} I_{\nu', \sigma'}}(\omega) = 2 \int_{-\infty}^{\infty} dt e^{i\omega t} [\langle I_{\nu, \sigma}(t) I_{\nu', \sigma'}(0) \rangle - \langle I_{\nu, \sigma} \rangle \langle I_{\nu', \sigma'} \rangle]. \quad (10)$$

For the symmetric coupling, which we consider in this paper, $S_{I_{L, \sigma} I_{L, \sigma'}}(\omega) = S_{I_{R, \sigma} I_{R, \sigma'}}(\omega) = 2I_{\sigma} \delta_{\sigma, \sigma'} + S_{I_{L, \sigma} I_{R, \sigma'}}(\omega) = S_{\sigma, \sigma'}$ where the $2I_{\sigma} \delta_{\sigma, \sigma'}$ term is the classical Schottky noise^{18,38}. The spin current shot noise is defined as

$$S^{(s)} = s^2 (S_{\uparrow, \uparrow} + S_{\downarrow, \downarrow} - S_{\uparrow, \downarrow} - S_{\downarrow, \uparrow}). \quad (11)$$

The photo-current shot noise, $S^{(ph)}$, is defined the same way as $S_{I_{\nu, \sigma} I_{\nu', \sigma'}}(\omega)$ with the substitution $I_{\nu, \sigma} \rightarrow I_{photon}$. Here we use the approach we developed in Ref. 38 to evaluate the shot noise.

The zero frequency spin shot noise as a function of the Rabi frequency behaves similarly for both the quantum and classical fields (Fig. 3(b)). In the semiclassical case, we obtained for the zero frequency noise

$$S^{(s)}/2sI_s = (3\Gamma^4 + 2\Gamma^2 R_{rf}^2 + 19R_{rf}^4)/2(\Gamma^2 + 3R_{rf}^2)^2. \quad (12)$$

For weak coupling, $G, R_{rf} \ll \Gamma$, the shot noise is super-Poissonian, approaching $3/2$ as $G, R_{rf} \rightarrow 0$. Increasing the dot-field coupling decreases the noise until the noise plateaus for $G, R_{rf} \gg \Gamma$. The plateau value is $\simeq 2sI_s$ for the classical field but for the quantum field it becomes increasingly sub-Poissonian for increasing Γ_{cav} .

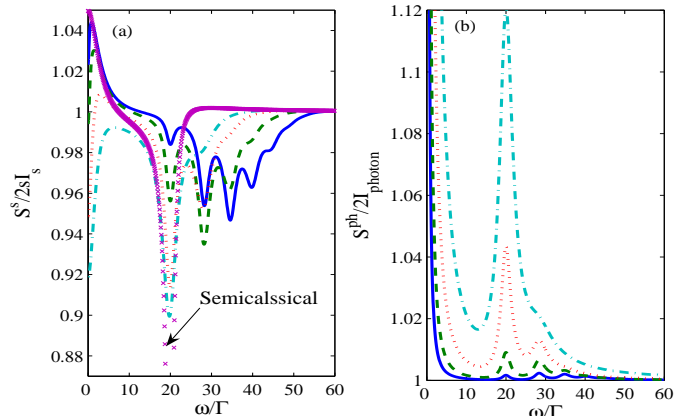


FIG. 4: The frequency dependent spin current (a) and photon (b) shot noise vs. frequency for $R_{rf} = G = 10\Gamma$ and different Γ_{cav} (curve labels same as Fig. 2).

The frequency dependent shot noise provides even more information as can be seen in Fig. 4. For strong coupling, $G \gg \Gamma, \Gamma_{cav}$, dips (peaks) are present in the spin (photon) current noise spectrum, which are located precisely at the cavity Rabi frequencies $2G\sqrt{n+1}$ for $n = 0, 1, 2, \dots$. By comparison $S^{(s)}(\omega)$ exhibits a single dip at $\omega = 2R_{rf}$ for the semiclassical system. These resonances in the noise spectrum represent a definite sign of the quantization of the cavity field. For $\Gamma_{cav} < \Gamma$ there is a large probability that more than one electron will tunnel through the dot before the photons start to leave the cavity. Whenever one electron passes through the dot, the number of photons increases by one. This process continues until the cavity starts to decay. For

$\Gamma_{cav} \ll \Gamma$, this will lead to a non-negligible probability for the cavity to be in a state with $n = 0, 1, 2, 3, \dots$ photons. Qualitatively, each one of these photon states will contribute to the shot noise spectrum with a weight $P(n)$, where $P(n)$ is the probability of having n photons, which is shown in the inset of Fig. 3(b). By increasing Γ_{cav} , the number of populated photon states decreases until finally for $\Gamma_{cav} \gg \Gamma$, only the dip (peak) at the vacuum Rabi frequency, $2G$, remains in the spectrum. We have fitted these dips to Lorentzians and found them to have a width of $\Gamma + (n+1)\Gamma_{cav}/2$ for $\Gamma_{cav} \leq \Gamma$. Decreasing G will decrease the separation between the dips (peaks) until they begin to overlap when $G \lesssim \Gamma, \Gamma_{cav}$.

IV. CONCLUSION

In conclusion, we have studied the spin current and spin current shot noise generated by a quantum dot coupled to single mode of an optical microcavity. We found that the spin current can be significantly larger than for a classical driving field due to cavity decay of the quantized field. Most importantly, we showed that the spin current shot noise exhibits clear signatures of the discrete nature of the photon states in the cavity in the limit of strong cavity coupling.

Although no experiments have yet been performed studying transport through quantum dots embedded in cavities, it is very likely that the two avenues of research that have been pursued with self-assembled dots namely transport^{25,26,27} and cavity-QED^{21,22} will intersect in the near future. The main experimental challenge to such experiments are connecting metal electrodes to the devices, which are optically very absorbing and would lead to a strong reduction in the Q-factor of the cavity²⁴. This might be ameliorated by using electrodes consisting of doped semiconductors with carrier concentrations below that of metals. On the other hand, the enhancement of the spin current over the semiclassical limit should be observable even with a low-Q cavity.

¹ Igor Zutic, Jaroslav Fabian, S. Das Darma, Rev. Mod. Phys. **76**, 323 (2004).
² M. A. M. Gijs and G. E. W. Bauer, Adv. Phys. **46**, 285 (1997).
³ M. I. D'yakonov and V. I. Perel', JETP Lett. **13**, 467 (1971); J. E. Hirsch, Phys. Rev. Lett. **83**, 1834 (1999); S. Zhang, Phys. Rev. Lett. **85**, 393 (2000); T. P. Pareek, Phys. Rev. Lett. **92**, 076601 (2004).
⁴ S. Murakami, N. Nagaosa, and S.-C. Zhang, Science **301**, 1348 (2003); J. Sinova *et al.*, Phys. Rev. Lett. **92**, 126603 (2004); Branislav K. Nikolić, Liviu P. Zârbo, and Satofumi Souma, Phys. Rev. B **72**, 075361 (2005).
⁵ E. I. Rashba, Physica E (Amsterdam) **20**, 189 (2004).
⁶ M. J. Stevens *et al.*, Phys. Rev. Lett. **90**, 136603 (2003); R. D. R. Bhat and J. E. Sipe, Phys. Rev. Lett. **85**, 5432 (2000).

⁷ E. R. Mucciolo, C. Chamon, and C. M. Marcus, Phys. Rev. Lett. **89**, 146802 (2002).
⁸ Susan K. Watson, R. M. Potok, and C. M. Marcus, and V. Umansky, Phys. Rev. Lett. **91**, 258301 (2003).
⁹ P. Sharma and C. Chamon, Phys. Rev. Lett. **87**, 096401 (2001); R. Citro, N. Andrei, Q. Niu, Phys. Rev. B **68**, 165312 (2003).
¹⁰ R. Benjamin and C. Benjamin, Phys. Rev. B **69**, 085318 (2004).
¹¹ M. Blaauboer and C. M. L. Fricot, Phys. Rev. B **71**, 041303(R).
¹² E. Sela and Y. Oreg, Phys. Rev. B **71**, 075322 (2005).
¹³ Yanxia Xing *et al.*, Phys. Rev. B **70**, 245324 (2004); M. Yang and S. S. Li, Phys. Rev. B **70**, 195341 (2004); A. Brataas and Y. Tserkovnyak, Phys. Rev. Lett. **93**, 087201 (2004); C. Benjamin and R. Citro, Phys. Rev. B **72**,

- 085340.
- ¹⁴ B. G. Wang *et al.*, Phys. Rev. B **67**, 92408 (2003); P. Zhang *et al.*, Phys. Rev. Lett. **91**, 196602 (2003).
- ¹⁵ Bing Dong, H. L. Cui, and X. L. Lei, Phys. Rev. Lett. **94**, 066601 (2005).
- ¹⁶ O. Sauret and D. Feinberg, Phys. Rev. Lett. **92**, 106601 (2004).
- ¹⁷ Baigeng Wang, Jian Wang, and Hong Guo, Phys. Rev. B **69**, 153301 (2004).
- ¹⁸ Ya.M. Blanter and M. Büttiker, Phys. Rep. **336**, 1 (2000); C. Beenakker and C. Schönberger, Phys. Today, May 2003, **37** (2003)
- ¹⁹ Pierre Meystre and Murray Sargent, *Quantum Optics, 3rd Ed.* (Springer-Verlag, Berlin, 1998).
- ²⁰ H. J. Kimble, M. Dagenais, and L. Mandel, Phys. Rev. Lett. **39**, 000691 (1977).
- ²¹ J. P. Reithmaier *et al.*, Nature **432**, 197 (2004); T. Yoshie *et al.*, Nature **432**, 200 (2004).
- ²² E. Peter *et al.* Phys. Rev. Lett. **95**, 067401 (2005).
- ²³ W. G. van der Wiel *et al.* Rev. Mod. Phys. **75**, 1 (2003).
- ²⁴ Stefan Strauf, personal communication.
- ²⁵ K. H. Schmidt, M. Versan, U. Kunze, D. Reuter, and A. D. Wieck, Phys. Rev. B **62**, 15879 (2000).
- ²⁶ T. Ota *et al.*, Phys. Rev. Lett. **93**, 066801 (2004).
- ²⁷ P. Barthold, Phys. Rev. Lett. **96**, 246804 (2006).
- ²⁸ D. Heis, M. Kroutvar, J. J. Finley, and G. Abstreiter, Solid State Communications **135**, 591 (2005); H. Drexler *et al.*, Phys. Rev. Lett. **73**, 2252 (1994); R. J. Warburton *et al.*, Nature **405**, 926 (2000).
- ²⁹ M. Atatüre *et al.*, Science **312**, 551 (2006).
- ³⁰ We use the level structure defined in Ref. [11] rather than the conventions used in Refs. [9] and [14] where the spin down state has lower energy than the spin up state.
- ³¹ A. Imamoglu *et al.*, Phys. Rev. Lett. **83**, 4204 (1999).
- ³² Pochung Chen, C. Piermarocchi, L. J. Sham, D. Gammon, D. G. Steel, Phys. Rev. B **69**, 075320 (2004).
- ³³ A. Greilich *et al.*, Phys. Rev. Lett. **96**, 227401 (2006).
- ³⁴ M. V. Gurudev Dutt *et al.*, Phys. Rev. Lett. **94**, 227403 (2005).
- ³⁵ Bing Dong, H. L. Cui, and X. L. Lei, Phys. Rev. B **69**, 035324 (2004).
- ³⁶ J. M. Elzerman *et al.* Nature **430**, 431 (2004).
- ³⁷ R. Hanson, L. H. Willems van Beveren, I. T. Vink, J. M. Elzerman, W. J. M. Naber, F. H. L. Koppens, L. P. Kouwenhoven, and L. M. K. Vandersypen, Phys. Rev. Lett. **94**, 196802 (2005); R. Hanson, L. M. K. Vandersypen, L. H. Willems van Beveren, J. M. Elzerman, I. T. Vink, and L. P. Kouwenhoven, Phys. Rev. B **70**, 241304(R) (2004).
- ³⁸ Ivana Djuric, Bing Dong, H. L. Cui, J. Appl. Phys. **99**, 063710 (2006).
- ³⁹ Wei Lu *et al.*, Nature **423**, 422 (2003).
- ⁴⁰ J. McKeever *et al.*, Nature **425**, 268 (2003).